

Star-Shaped Push-Pull Compounds Having 1,3,5-Triazine Cores

Herbert Meier,^{*[a]} Elena Karpuk,^[a] and Hans Christof Holst^[a]**Keywords:** Absorption / Conjugation / Protonation / Push-pull effects

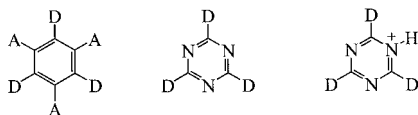
The 1,3,5-triazines **9–11** having OPV chains in the 2-, 4- and 6-position represent star-shaped compounds which exhibit strong push-pull effects. Their long-wavelength absorption $S_0 \rightarrow S_1$ is characterized by an intramolecular charge transfer (ICT) from the dialkylamino group as electron donor D via the conjugated chain to the 1,3,5-triazine core as electron acceptor A. Protonation of the dialkylamino group removes the donor capability, whereas protonation of the 1,3,5-triazine ring enhances the acceptor strength. Thus, the prevailing protonation site has a crucial influence on the push-pull effect and the ICT. The transition energies ΔE ($S_0 \rightarrow S_1$) pass

through a minimum for the second generation **10** in the electroneutral series **9–11**; on the contrary they pass through a maximum for **10b** in the protonated series **9a**, **10b**, **11b**. These unexpected results are explained by the superposition of different effects, namely the extension of the conjugation from **9** to **11**, the decreasing ICT for growing distances of D and A, the aggregation, and the positions of the protonation in the presence of increasing amounts of CF_3COOH .

(© Wiley-VCH Verlag GmbH & Co. KGaA, 69451 Weinheim, Germany, 2006)

Introduction

Conjugated oligomers with donor–acceptor substitution attract a great deal of attention because they represent interesting materials for various applications in materials science.^[1–5] The push-pull effect can be realized in conjugated linear chains by terminal substitution with a donor group D and an acceptor group A. A further structure concept is based on star-shaped compounds whose arms bear (alternatingly) donor and acceptor functionalities.^[1,2] Benzene ring systems with three donor groups D and three acceptor groups A, which are linked directly or through a conjugated spacer to the core, are typical examples.^[6,7] The acceptor functions can be discerned by nitrogen atoms as well, when a 1,3,5-triazine core is used (Scheme 1).



Scheme 1. Push-pull-substituted benzene systems with D_{3h} symmetry, corresponding donor-substituted 1,3,5-triazines and their tautomeric 1,3,5-triazinium ions showing a fast automerization.

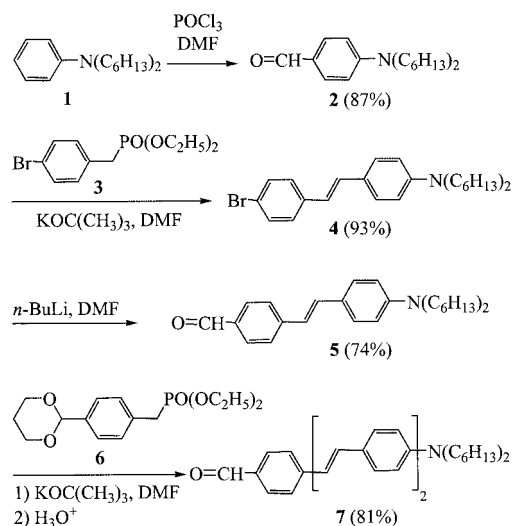
Some time ago we reported on the preparation and the properties of 2,4,6-tristyryl-1,3,5-triazines and their higher homologues having oligo(1,4-phenylenevinylene) [OPV] chains.^[8–10] We are studying now star-shaped systems with a 1,3,5-triazine core and three OPV chains which bear ter-

minal dialkylamino groups. This structure concept conveys the compounds an octupolar character with a strong push-pull effect in each of the three arms. Such systems promise outstanding properties in nonlinear optics (NLO), two-photon absorption (TPA) and two-photon excited fluorescence (TPEF).^[11]

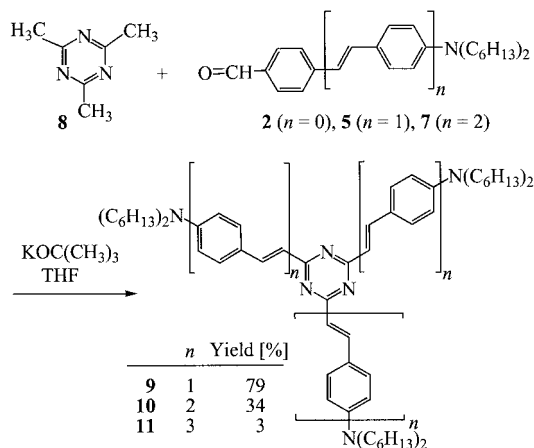
Results and Discussion

The synthetic strategy for the preparation of 1,3,5-triazines with three OPV chains in 2-, 4- and 6-position is based on threefold condensation reactions of 2,4,6-trimethyl-1,3,5-triazine and corresponding aldehydes. Vilsmeier formylation of *N,N*-dihexylaniline (**1**) gives 4-(dihexylamino)benzaldehyde (**2**) in high yields (Scheme 2). Subsequent Wittig–Horner reaction of **2** and diethyl 4-bromobenzylphosphonate (**3**) affords the (*E*)-stilbene **4**. The bromo substituent in **4** can be replaced by a formyl group by applying a Bouveault process with *n*-BuLi/DMF. Thus, the aldehyde **5** is obtained from **1** in three steps with an overall yield of 60%. The phosphonate **6** serves then for the extension of the conjugated chain. Wittig–Horner reaction of **5** and **6** yields directly the aldehyde **7**, because the protecting 1,3-dioxane group in **6** is cleaved in the work-up of the Wittig–Horner process. Diethyl 4-[1,3-dioxan-2-yl]benzyl phosphonate (**6**) is a very useful reagent to extend the conjugated chain of OPV aldehydes. The reaction of **2** and **6** leads in a one-step process to **5**; however, the overall yield for **1**→**2**→**5** is somewhat lower than 60%. The (*E*) selectivity of the Horner variant is generally high in the stilbenoid series so that (*Z*) configurations can not be detected in the solid products **5** and **7**. The detection limit in 1H and ^{13}C NMR spectroscopy amounts to about 3%.

[a] Institut für Organische Chemie der Johannes Gutenberg Universität, Duesbergweg 10–14, 55099 Mainz, Germany
Fax: +49-6131-3925396
E-mail: hmeier@mail.uni-mainz.de

Scheme 2. Preparation of the aldehydes **2**, **5** and **7**.

The three “homologous” aldehydes **2**, **5** and **7** are then condensed in an alkaline medium with 2,4,6-trimethyl-1,3,5-triazine (**8**). The yield is high for the smallest system **9**, moderate for **10** with longer side chains, and poor for **11**, which has the longest side chains. ^1H NMR reaction spectra show that the first two condensation processes work reasonably well; however, the third process proved to be difficult – in particular for the longer aldehydes **5** and **7**. The hexyl chains on the amino groups guarantee a good solubility of the target compounds^[12] (see Scheme 3).

Scheme 3. Preparation of the star-shaped compounds **9–11** having a 1,3,5-triazine core and three OPV chains with dihexylamino groups as electron-donor groups in the terminal positions.

The long-wavelength absorption data of **9–11** are listed in Table 1. As the band does not have a fine structure, which allows the determination of the $0 \rightarrow 0$ transition, the $\lambda_{0,1}$ values are taken with $\epsilon(\lambda_{0,1}) = 0.1\epsilon(\lambda_{\max})$ at the long-wavelength foot of the band. Both values λ_{\max} as well as $\lambda_{0,1}$ show the same behavior in the series **9–11**, namely an increase of the values from **9** to **10** and then a decrease to **11**.

Table 1. UV/Vis absorption of the compounds **9–11** measured in diluted solutions ($c \leq 10^{-5}$ M) in CH_2Cl_2 .

Compound	λ_{\max} [nm]	$\lambda_{0,1}$ [nm] ^[a]	ϵ_{\max} [$\text{cm}^2 \text{mmol}^{-1}$]
9	442	488	131870
10	457	530	435385
11	442	522	138990 ^[b]

[a] Wavelength, where $\epsilon = 1/10 \epsilon_{\max}$. [b] Very broad band.

The charge-transfer character of the band becomes evident by the absorption in the visible region. 2,4,6-Tris[(*E*-styryl)-1,3,5-triazine has a λ_{\max} value in the UV at 327 nm.^[8] However, the intramolecular charge transfer (ICT) depends strongly on the distance of donor D and acceptor A. The transition energy ΔE ($S_0 \rightarrow S_1$) of push-pull oligomers is lowered by the extension of the conjugation and by the ICT. Both effects are superimposed and can lead to four different functions $\lambda_{\max}(n)$, where n represents the number of repeat units in a conjugated oligomer series:^[1,5]

- $\Delta E(n+1) < \Delta E(n)$ monotonous bathochromic shift
- $\Delta E(n+1) > \Delta E(n)$ monotonous hypsochromic shift
- $\Delta E(n+1) \approx \Delta E(n)$ borderline case between a) and b)
- ΔE goes through a minimum for a certain n' .

The fifth thinkable case, in which ΔE passes a maximum for a special n' , is still unknown.

The present series **9–11** belongs to category d). The decrease of the ICT with increasing n provokes a hypsochromic effect, which can not be compensated for $n = 2$ by the bathochromic effect caused by the extension of the conjugation (growing values n). This result is in contrast to the analogous star-shaped oligomers with a 1,3,5-triazine core and three OPV arms with terminal alkoxy groups which belong to category a).^[8] Alkoxy groups are weaker electron donors than dialkylamino groups; therefore the extension of the chromophores (increasing numbers n) can overcompensate the decrease of the ICT.

The absorption of **9–11** depends unusually strong on the concentration. Figure 1 demonstrates this effect for the range between $c_1 = 1.29 \cdot 10^{-5}$ and $c_5 = 2.26 \cdot 10^{-4}$ M solutions of **11** in CH_2Cl_2 . Doubling of the concentration in each of the four steps from c_1 to c_5 does not result in a doubling of the A_{\max} values. Moreover, λ_{\max} changes from 441 to 486 nm. From $c_3 = 5.15 \cdot 10^{-5}$ M on, the effect on A_{\max} and λ_{\max} becomes very pronounced. Obviously Lambert–Beer’s law is not valid. The change of the band shape gives the impression, that for increasing concentrations more and more aggregates absorb, which have the character of J aggregates with higher λ_{\max} values but lower A_{\max} (ϵ_{\max}) values. The compounds **9** and **10** exhibit the same behavior. The ϵ_{\max} values, listed in Table 1, refer to concentrations of $10^{-5} \text{ mol} \cdot \text{L}^{-1}$ or less. Further dilution changes the ϵ_{\max} values to a minor extent; the ϵ_{\max} value of **11** varies for example from 128020 to 138990 $\text{cm}^2 \text{mmol}^{-1}$ on going from $1.028 \cdot 10^{-5}$ M to $2.57 \cdot 10^{-6}$ M solutions in CH_2Cl_2 . One can imagine, that the disc-like molecules **9–11** form aggregates, in which the 1,3,5-triazine core of the molecule is superimposed by an amino group of the next molecule, etc. Thus,

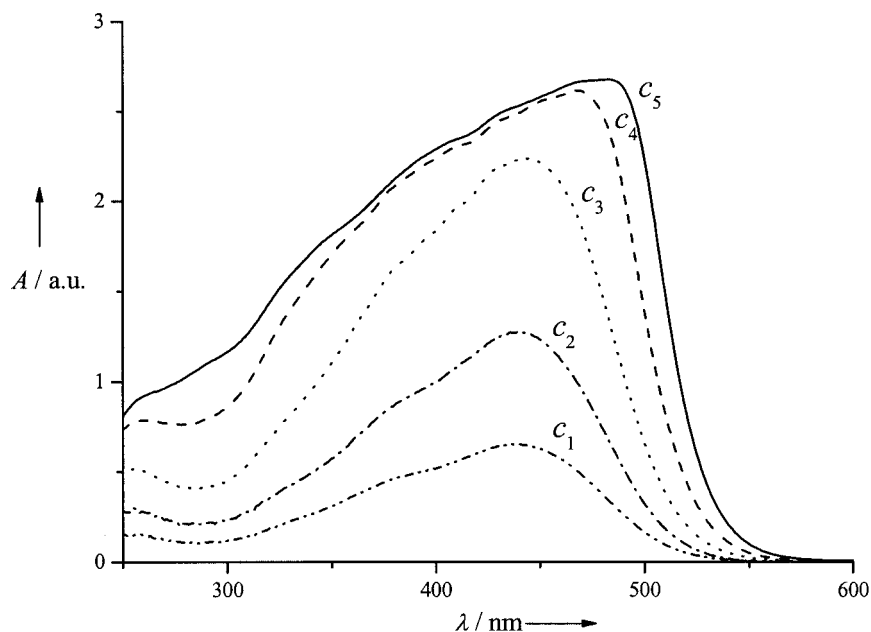
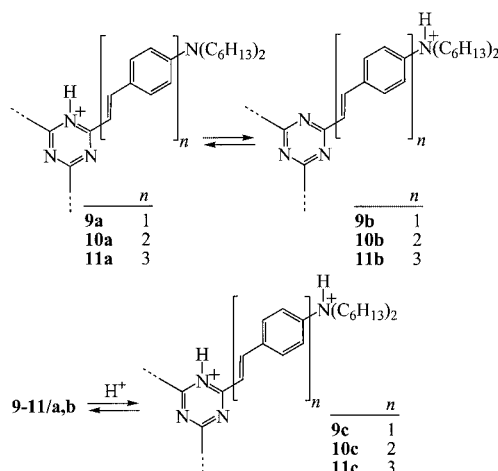


Figure 1. Long-wavelength absorption of compound **11** at increasing concentrations in CH_2Cl_2 : $c_1 = 1.29 \cdot 10^{-5}$, $c_2 = 2.58 \cdot 10^{-5}$, $c_3 = 5.15 \cdot 10^{-5}$, $c_4 = 1.03 \cdot 10^{-4}$, and $c_5 = 2.26 \cdot 10^{-4} \text{ mol} \cdot \text{L}^{-1}$.

additional to the intramolecular push-pull effect, an intermolecular charge transfer can occur. However, a very regular self-organization, which provokes discotic mesophases, could not be observed in the DSC.

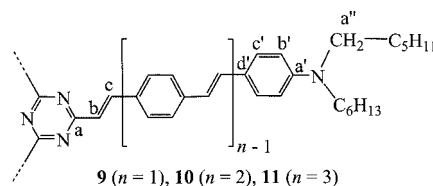
An important point concerns now the influence of protonating media. Protonation of the amino groups should lead to the disappearance of their donor character, whereas protonation of the 1,3,5-triazine ring should enhance the acceptor capability. Thus, protonation can weaken or strengthen the push-pull effect – depending on the preferred side. Scheme 4 depicts the equilibria of the protonated compounds **9–11**.



Scheme 4. Equilibria of the protonated compounds of **9–11** in $\text{CH}_2\text{Cl}_2/\text{CF}_3\text{COOH}$.

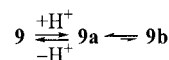
The ^{13}C NMR spectra provide a reliable tool for the observation of partial charges and their changes by protonation. Figure 2 shows the alteration of the signals by ad-

dition of CF_3COOH to a solution of **9** in CD_2Cl_2 . The assignment of the signals is based on HMQC and HMBC measurements. Scheme 5 contains the descriptors for the carbon atoms in **9–11**.



Scheme 5. Carbon atoms in **9–11**, selected for the determination of the protonation side.

Protonation of **9** does not change the C_3 symmetry axis valid in the NMR spectra; that means a fast exchange of protons has to be assumed. A comparison of parts a and b of Figure 2 reveals very small low-field shifts for a'', a', b', and d', the carbon atoms on the donor side, and big shifts for a ($\Delta\delta = -4.4$ ppm), b ($\Delta\delta = -7.1$ ppm) and c ($\Delta\delta = +7.2$ ppm) on the acceptor side. In particular the polarization of the olefinic double bond is strongly enhanced. The difference $\delta(c) - \delta(b)$ increases from 20.4 to 34.7 ppm. These findings demonstrate that the initial protonation, obtained for the molar ratio $\mathbf{9}/\text{CF}_3\text{COOH} = 1:2.8$, preferentially takes place on the 1,3,5-triazine ring. Normally tertiary amines are much more basic than 1,3,5-triazines. The strong push-pull effect in **9** reverts obviously the situation.



Further protonation to **9c** (molar ratio $\mathbf{9}/\text{CF}_3\text{COOH} = 1:86$) occurs then on the amino nitrogen atoms. Considerable down-field shifts are observed (see part c of Figure 2) for the carbon atoms a'' ($\Delta\delta = +8.0$ ppm), b' ($\Delta\delta =$

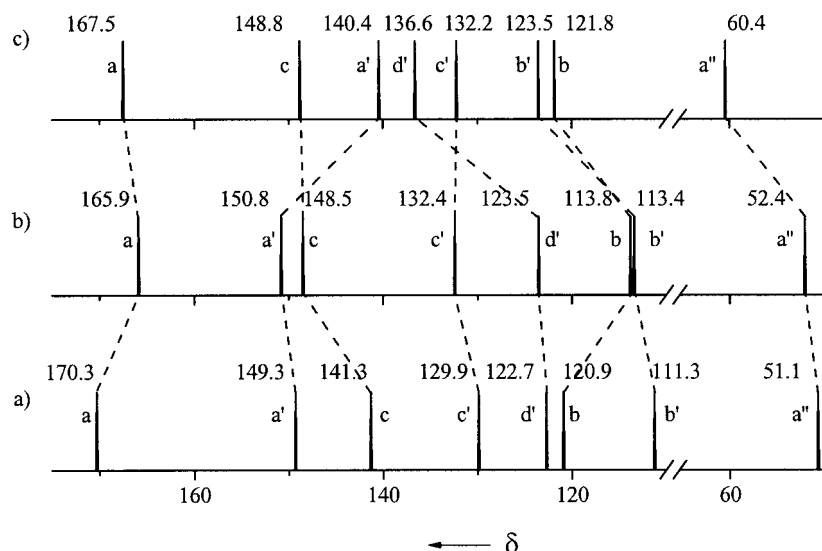
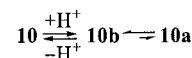


Figure 2. ^{13}C NMR signals of **9** and their shift caused by protonation: a) $3.24 \cdot 10^{-2}$ M solution of **9** in 0.75 mL CD_2Cl_2 ; b) addition of 5 μL ($6.73 \cdot 10^{-5}$ mol) CF_3COOH ; c) addition of 155 μL ($2.09 \cdot 10^{-3}$ mol) CF_3COOH .

+10.1 ppm), d' ($\Delta\delta = +13.1$ ppm) and b ($\Delta\delta = +8.0$ ppm). The polarization of the olefinic double bond in **9c** [$\delta(c) - \delta(b) = 27.0$ ppm] is between that of **9a** and the unprotonated compound **9**. All other carbon signals with the exception of a' are less affected by the additional protonation. A comparison of parts a and c of Figure 2 demonstrates unambiguously that both positions are protonated in **9c**. The decrease of the electron density by changed mesomeric effects in the position b' and c becomes evident by strong down-field shifts. A proton exchange mechanism, which is fast in the sense of the NMR time scale, keeps the D_{3h} symmetry of **9** intact in the protonated species **9a,c**.

Figure 3 demonstrates the protonation of **10**. The same carbon atoms were selected as for **9** (Scheme 5), but the observed signal shifts caused by protonation are widely dif-

ferent. Addition of a small portion of CF_3COOH (molar ratio **10**/ CF_3COOH = 1:1.4) provokes strong down-field shifts of a'' ($\Delta\delta = +6.9$ ppm) and b' ($\Delta\delta = +9.5$ ppm) and an up-field shift of a' ($\Delta\delta = -5.0$ ppm). Accordingly, protonation preferentially takes place at the donor end; structure **10b** predominates in the equilibrium.



The larger distance $D-A$ in **10** (compared to **9**) reduces the push-pull effect and changes consequently the electron density to such an extent, that the amine basicity prevails – as a priori expected for the whole series. Further protonation to **10c** (molar ratio **10**/ CF_3COOH = 1:10.5) occurs than on the 1,3,5-triazine nitrogen atoms. A strong down-

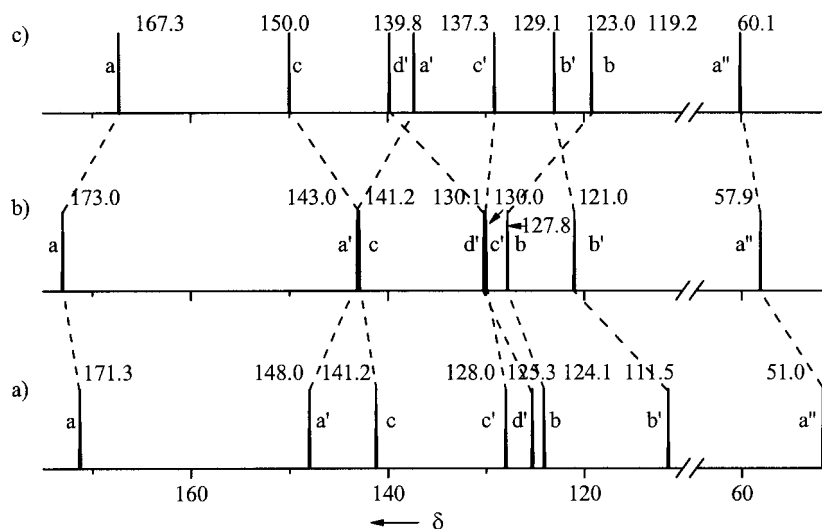
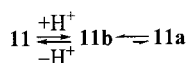


Figure 3. ^{13}C NMR signals of **10** and their shift caused by protonation: a) $1.29 \cdot 10^{-2}$ M solution of **10** in 0.75 mL CD_2Cl_2 ; b) addition of 1 μL ($1.35 \cdot 10^{-5}$ mol) CF_3COOH ; c) addition of 7.5 μL ($10.10 \cdot 10^{-5}$ mol) CF_3COOH .

field shift (Figure 3, c) of signal c ($\Delta\delta = +7.1$ ppm) and a strong up-field shift of b ($\Delta\delta = -8.6$ ppm) are good indications for this effect.

Compound **11** has an even larger distance D–A than **10** and consequently an even weaker push-pull character. The protonation effects on the ^{13}C chemical shifts are similar to those observed for **10**. Initial protonation shifts a'' and b' down-field and a' up-field.



Further protonation to **11c** occurs than on the nitrogen atoms of the 1,3,5-triazine ring, indicated for example by the up-field shift of carbon a by 4.4 ppm. The exchange mechanism, which establishes the D_{3h} symmetry is in **11b,c** somewhat slower than in **10b,c**, so that the NMR signals are broader in **11b,c**.

The NMR results are important to understand the UV/Vis spectra of **9–11/a–c**. The yellow solution of **9** in CH_2Cl_2 turns first red on addition of CF_3COOH , then violet and finally almost colorless (Figure 4). When the molar ratio **9**/ CF_3COOH = 1:2.8, used for the NMR measurement shown in part b of Figure 2, is kept constant for different concentrations of **9**, one recognizes, that the violet color is owing to protonated aggregates of **9**. Figure 5 shows that a new absorption band between 500 and 600 nm emerges, whose relative intensity increases with increasing concentration of **9**. The preliminary aggregation model, mentioned before, is in accordance with this result, since the intermolecular charge transfer between the dialkylamino group and the 1,3,5-triazine ring should be even more favored, when the 1,3,5-triazine ring is protonated.

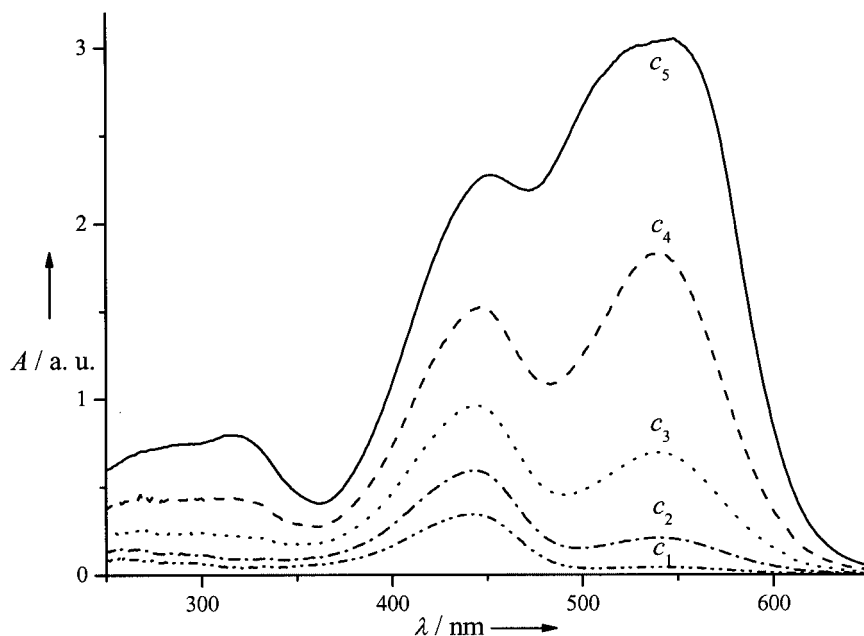


Figure 5. Long-wavelength absorption of **9** in $\text{CH}_2\text{Cl}_2/\text{CF}_3\text{COOH}$ for a constant molar ratio **9**/ CF_3COOH = 1:2.8 and different concentrations of **9**: $c_1 = 2.55 \cdot 10^{-6}$, $c_2 = 5 \cdot 10^{-6}$, $c_3 = 1.02 \cdot 10^{-5}$, $c_4 = 2.04 \cdot 10^{-5}$, $c_5 = 4.08 \cdot 10^{-5}$ mol \cdot L $^{-1}$.



Figure 4. Color change of a $2.44 \cdot 10^{-5}$ M solution of **9** in CH_2Cl_2 by addition of CF_3COOH .

When the molar ratio **9**/ CF_3COOH reaches 1:55, the new band reaches a λ_{max} value of 564 nm. Further addition of CF_3COOH does not change this value anymore, but the intensity of the band decreases continuously from then on and another new absorption band emerges at $\lambda_{\text{max}} = 326$ nm (molar ratio **9**/ CF_3COOH = 1:276). An even larger excess of CF_3COOH (molar ratio 1:1930) finally provokes an almost complete disappearance of the band at 564 nm, and a new maximum appears at 373 nm. Figure 6 demonstrates this effect which corresponds to the color change in Figure 4.

The interpretation of this behavior takes advantage of the NMR results. Protonation occurs first at the 1,3,5-triazine ring. The push-pull effect is enhanced and consequently the bathochromic shift of the charge-transfer band increased.^[1] Further protonation occurs then on the nitrogen atoms of the amino groups. In this situation, the overall

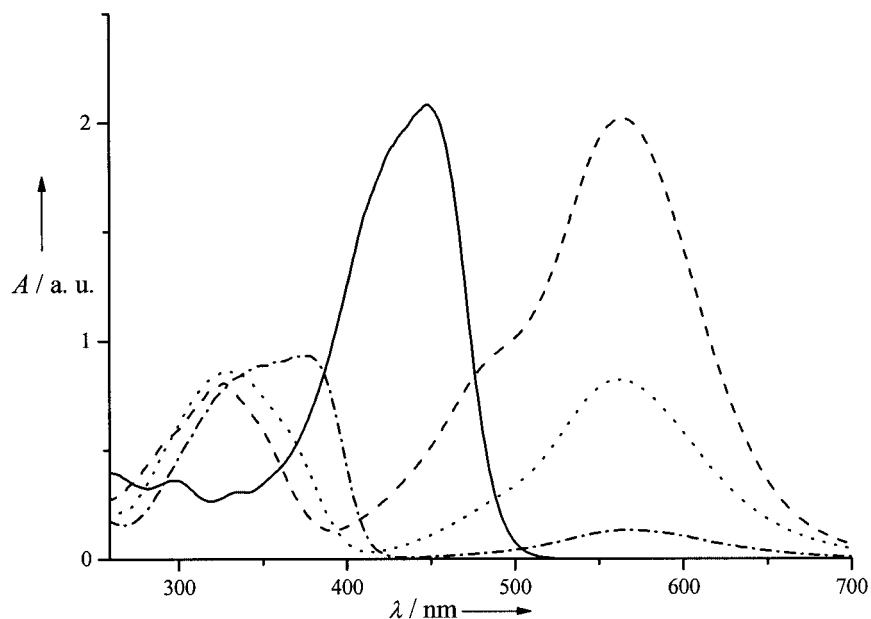


Figure 6. Absorbance of a $2.44 \cdot 10^{-5}$ M solution of **9** in CH_2Cl_2 (10 mL): neutral, ---- with $1 \mu\text{L}$ ($1.35 \cdot 10^{-5}$ mol) CF_3COOH , ···· with $5 \mu\text{L}$ ($6.73 \cdot 10^{-5}$ mol) CF_3COOH , - · - · - with $35 \mu\text{L}$ ($47.12 \cdot 10^{-5}$ mmol) CF_3COOH .

ICT is lost, and ions are generated with smaller charge transfers from the stilbene unit to the ammonium group and also in the opposite direction from the stilbene unit to the triazinium core.

The higher “generation” **10** behaves totally different (Figure 7). The very first protonation causes already a hypsochromic shift in so far as the band with $\lambda_{\text{max}} = 457$ nm decreases, and a new band with $\lambda_{\text{max}} = 394$ nm emerges. The relative height of the two bands depends on the concentration, when the molar ratio **10**/ CF_3COOH is kept con-

stant; that means aggregation plays here a role, too. Continuing protonation leads then to a bathochromic shift. A high excess of CF_3COOH gives rise to a strong band with a λ_{max} value of 451 nm, which is similar to the original band of unprotonated **10**. The molar ratios **10**/ CF_3COOH amount to 1:–, 1:11.6, 1:155 and 1:774 for the measurements depicted in Figure 7.

Whereas protonation of **9** leads first to a *bathochromic* shift and then to a *hypsochromic* shift, **10** behaves vice versa, initial protonation causes a *hypsochromic* shift, which is

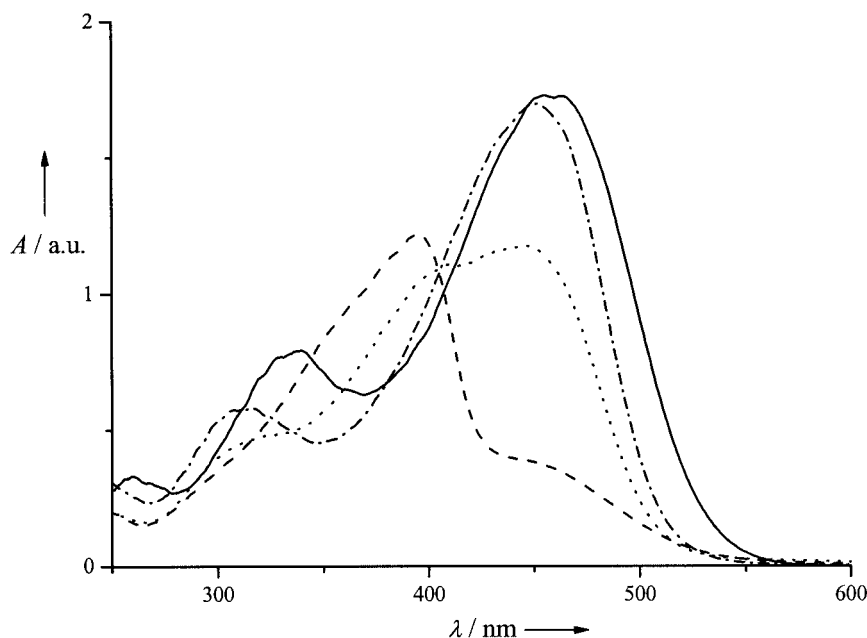


Figure 7. Absorbance of a $1.74 \cdot 10^{-5}$ M solution of **10** in CH_2Cl_2 (10 mL): neutral, ---- with $0.15 \mu\text{L}$ ($0.20 \cdot 10^{-5}$ mmol) CF_3COOH , ···· with $2 \mu\text{L}$ ($2.69 \cdot 10^{-5}$ mmol) CF_3COOH , - · - · - with $10 \mu\text{L}$ ($13.46 \cdot 10^{-5}$ mmol) CF_3COOH .

then followed by a *bathochromic* shift. The shifts observed in the UV/Vis spectra of **10** are smaller than those of **9**.

The third “generation” **11** resembles **10**. Protonation of **11** leads first to a hypsochromic effect, λ_{max} decreases from 440 nm to 412 nm (Figure 8). Further protonation causes then a bathochromic effect of the long-wavelength band to $\lambda_{\text{max}} = 485$ nm. The difference to the spectra of **10** is due to the fact, that a high excess of CF_3COOH causes a stronger bathochromic effect, so that the band surpasses the original maximum at 440 nm. The molar ratios of the measurements depicted in Figure 8 amount to **11**: $\text{CF}_3\text{COOH} = 1:-, 1:29.8, 1:89, 1:298$.

The absorption curves depicted in the Figures 6, 7, and 8 were selected from many measurements with different concentrations of **9–11** and of CF_3COOH in order to make the effects particularly clear. Each curve corresponds to the sum of absorptions of all species which are present in the equilibria. The exchange mechanisms, which were important for the NMR interpretation, do not play a role here, but the preferred protonation sites are of course the same in both spectroscopical measurements.

The extension of the conjugation in the series of the neutral compounds **9**, **10**, **11** is connected with a transition energy ΔE ($S_0 \rightarrow S_1$), which proceeds through a minimum for **10**, whereas ΔE for the initially protonated species **9a**, **10b**, **11b** proceeds through a maximum for **10b**. The finally protonated species **9c–11c** represent a bathochromic series whose red shift is mainly due to the extension of the chromophore.

The push-pull effect in each arm of **9–11** decreases with increasing length of the three arms. The same effect can be expected for the ICT. Figure 9 visualizes the energies for the electronic transitions ΔE ($S_0 \rightarrow S_1$) in dependence of the number of OPV repeat units. The neutral series **9**, **10**, **11**

belongs to the category d) mentioned in the beginning – and not as a priori assumed to category a).^[1] The initial protonation seems to lead to the often searched but until now never found category in which ΔE passes with increasing n through a maximum.^[1,5] But in reality this statement is not correct, because the site of protonation changes within the series **9a**, **10b**, **11b**. The series of final protonation **9c**, **10c**, **11c** belongs to category a), increasing numbers n cause a monotonous decrease of ΔE .

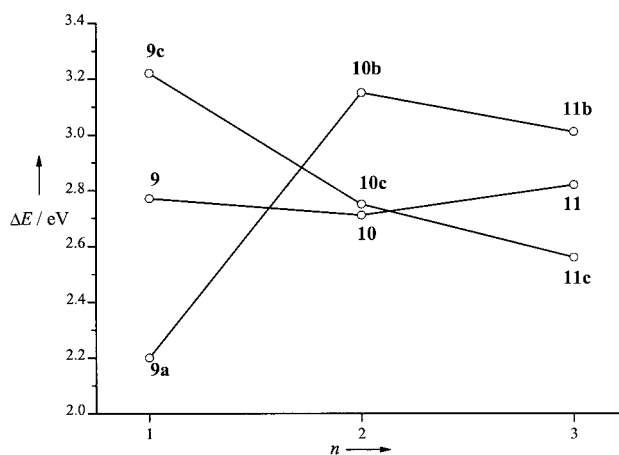


Figure 9. Energies ΔE of the electronic transition $S_0 \rightarrow S_1$ of the compounds **9–11** and their protonated species ($\text{CH}_2\text{Cl}_2/\text{CF}_3\text{COOH}$).

Apart from the linear optics, the 1,3,5-triazines **9–11** and their protonated species should show interesting nonlinear optics (NLO), in particular high β ($-2\omega; \omega, \omega$) values (second-order polarizabilities) can be expected. The NLO activity of such dipole-less compounds is due to large off-diagonal components of the second-order polarizability tensor.^[13–16] Until now only 1,3,5-triazines with small NLO

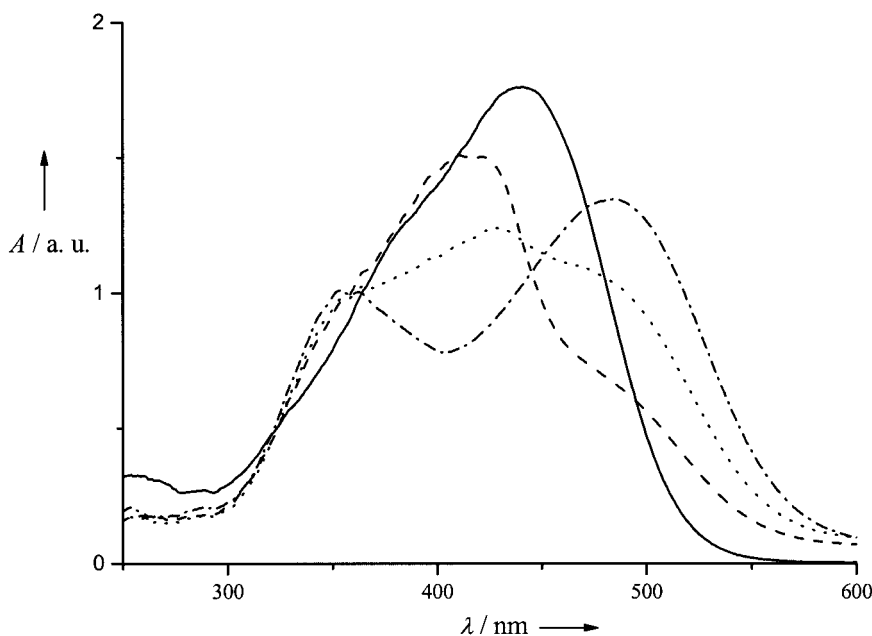


Figure 8. Absorbance of a $2.26 \cdot 10^{-5}$ M solution of **11** in CH_2Cl_2 (10 mL): neutral, ---- with 0.5 μL ($0.67 \cdot 10^{-5}$ mmol) CF_3COOH , ··· with 1.5 μL ($2.02 \cdot 10^{-5}$ mmol) CF_3COOH , - · - · with 5 μL ($6.73 \cdot 10^{-5}$ mmol) CF_3COOH .

chromophores were studied,^[17,18] but even these have very high β values. Since the β values in the appropriate three-level model^[17,18] increase with the product of the three transition dipoles and ΔE^2 , it will be highly interesting, how β (n) behaves in the series **9–11** and their protonated species.

Conclusions

The newly synthesized push-pull 1,3,5-triazines **9–11**, having OPV chains ($n = 1–3$) in 2-, 4- and 6-position and terminal dialkylamino groups exhibit an unusual absorption behavior ($S_0 \rightarrow S_1$) in neutral and protonating media ($\text{CH}_2\text{Cl}_2/\text{CF}_3\text{COOH}$). We assumed previously,^[1] that **9–11** ($n = 1–3$), as the corresponding compounds with OR instead of NR_2 groups,^[8] show a bathochromic shift of their long-wavelength absorption ($S_0 \rightarrow S_1$) with increasing numbers n . However, it turned out that ΔE ($S_0 \rightarrow S_1$) passes through a minimum for $n = 2$. This result is explained by the opposite effects, that ΔE (n) decreases with the extension of the conjugation (increasing n), but it increases with the reduction of the intramolecular charge transfer (ITC), when the distance of donor group (NR_2) and acceptor (1,3,5-triazine core) grows. Increasing protonation of **9** ($n = 1$) leads first to a strong *red shift* and then to a *blue shift*: the yellow solution in CH_2Cl_2 turns violet and then almost colorless. The homologues compounds **10** and **11** ($n = 2, 3$) behave opposite. Initial protonation provokes a *blue shift* and further protonation a *red shift*. The explanation for this unexpected result makes use of different protonation sites. Whereas **9**, having the strongest push-pull effect, is first protonated on the triazine ring (NMR proof), **10** and **11** are first protonated on an NR_2 group. Protonation on the triazine ring enhances the push-pull effect and the ICT, protonation on the NR_2 group decreases them. When both sides are protonated, the ICT becomes less important and the extension of the conjugation causes a *bathochromic shift*.

Experimental Section

General Remarks: UV/Vis: Zeiss MCS 320/340; CHCl_3 or CH_2Cl_2 as solvents. ^1H and ^{13}C NMR: Bruker Avance 600, AMX 400 and AC 300. CDCl_3/TMS as internal standard. MS: Finnigan MAT 95 (FD; accelerating voltage 5 kV), Micromass QTOF Ultima-3 (ESI, reference: CsI – NaI standard solution), DSC: Perkin – Elmer DSC 7. Melting points: Stuart Scientific SMP/3; uncorrected.

4-(Dihexylamino)benzaldehyde (2): POCl_3 (7.33 mL, 12.28 g, 0.08 mol) was slowly added to *N,N*-dihexylaniline (21.0 g, 0.08 mol) in DMF (18.5 mL, 17.52 g, 0.24 mol). The reaction mixture turned green on stirring at room temperature and was then heated to 80 °C for 3 h. After having poured it on crashed ice, the mixture was extracted with diethyl ether (3 × 50 mL). The unified organic phases were washed with saturated aqueous NaHCO_3 and H_2O and dried with Na_2SO_4 . Evaporation of the solvent led to an oil (19.5 g, 87%), which could be purified in small portions by column chromatography (20 × 3 cm SiO_2 , CH_2Cl_2). ^1H NMR (CDCl_3): $\delta = 0.87$ (t, 6 H, CH_3), 1.30 (m, 12 H, CH_2), 1.58 (m, 4 H, $\beta\text{-CH}_2$), 3.13 (t, 4 H, $\alpha\text{-CH}_2$), 6.61/7.67 (AA'MM', 4 H, arom. H), 9.67

(s, 1 H, CHO) ppm. ^{13}C NMR (CDCl_3): $\delta = 14.0$ (CH_3), 22.6, 26.7, 27.1, 31.6 (CH_2), 51.1 (NCH_2), 110.6 (C-3), 124.5 (C-1), 132.6 (C-2), 152.6 (C-4), 189.8 (CHO) ppm. FD MS: m/z (%) = 289 (100) [M^+]. $\text{C}_{19}\text{H}_{31}\text{NO}$ (289.5): calcd. C 78.84, H 10.79, N 4.84; found C 79.18, H 10.59, N 5.10.

4-[(E)-2-(4-Bromophenyl)vinyl]-N,N-dihexylaniline (4): Aldehyde **2** (4.74 g, 16.9 mmol) and diethyl 4-bromobenzylphosphonate (**3**)^[19,20] (5.19 g, 19.9 mmol) dissolved in dry DMF (150 mL) were degassed and slowly added whilst stirring in Ar to $\text{KOC}(\text{CH}_3)_3$ (5.71 g, 51.0 mmol) in dry DMF (150 mL). After 2 h at room temperature, the mixture was poured on crushed ice. The water layer was extracted CHCl_3 (3 × 50 mL) (eventually some NaCl was added), and the unified organic phases were dried with Na_2SO_4 . The volatile parts were evaporated and the residue filtered through SiO_2 (10 × 5 cm) with petroleum, b.p. 40–70 °C/ethyl acetate, 95:5. The obtained orange solid (6.95 g, 93%) showed in the DSC a melting point of 76.4 °C. It was identical with an authentic sample.^[21] ^1H NMR (CDCl_3): $\delta = 0.88$ (t, 6 H, CH_3), 1.30 (m, 12 H, CH_2), 1.57 (m, 4 H, $\beta\text{-CH}_2$), 3.26 (t, 4 H, $\alpha\text{-CH}_2$), 6.59/7.34 (AA'MM', 4 H, 2-H, 3-H, 5-H, 6-H), 6.78/6.99 (AB, $^3J = 16.2$ Hz, 2 H, olefin. H), 7.31/7.40 (AA'BB', 4 H, arom. H) ppm. ^{13}C NMR (CDCl_3): $\delta = 14.0$ (CH_3), 22.6, 26.8, 27.3, 31.7 (CH_2), 51.0 (NCH_2), 111.6 (C-2), 119.9 (C_qBr), 122.2, 129.6 (olefin. CH), 124.0 (C-4), 127.4, 131.6 (aromat. CH), 127.8 (C-3), 137.3 (aromat. C_q), 148.0 (C-1) ppm.

4-[(E)-2-(4-Dihexylaminophenyl)vinyl]benzaldehyde (5): A solution of *n*-BuLi (2.74 M) in hexane (8.4 mL, 23.0 mmol) was added with a syringe under Ar to **4** (6.77 g, 15.3 mmol), dissolved in dry diethyl ether (250 mL) at –10 °C. Stirring was continued for 30 min at this temperature till dry DMF (2.9 mL, 2.75 g, 37.9 mmol) was added. After 1 h at room temperature, H_2O (100 mL) was added. The organic layer was separated, extracted 2 times with the equivalent volume of H_2O , and dried with Na_2SO_4 . Column filtration (8 × 13 cm SiO_2 , petroleum b.p. 40–70 °C/ethyl acetate, 2:1) yielded 4.43 g (74%) of an orange solid, which melted at 75 °C. The product was identical with an authentic sample.^[22] ^1H NMR (CDCl_3): $\delta = 0.89$ (t, 6 H, CH_3), 1.31 (m, 12 H, CH_2), 1.58 (m, 4 H, $\beta\text{-CH}_2$), 3.27 (t, 4 H, $\alpha\text{-CH}_2$), 6.60/7.38 (AA'MM', 4 H, arom. H), 6.87/7.17 (AB, $^3J = 16.4$ Hz, 2 H, olefin. H), 7.56/7.80 (AA'BB', 4 H, 2-H, 3-H, 5-H, 6-H), 9.93 (s, 1 H, CHO) ppm. ^{13}C NMR (CDCl_3): $\delta = 14.0$ (CH_3), 22.7, 26.8, 27.3, 31.7 (CH_2), 51.0 (NCH_2), 111.5, 126.1 (aromat. CH), 121.9, 132.6 (olefin. CH), 123.8, 134.3, 144.8, 148.4 (aromat. C_q), 128.4 (C-3), 130.2 (C-2), 191.6 (CHO) ppm. MS ESI: m/z (%) = 392 (100) [$\text{M} + \text{H}$]⁺.

4-((E)-2-{4-[(E)-2-(4-Dihexylaminophenyl)vinyl]phenyl}vinyl)benzaldehyde (7): $\text{KOC}(\text{CH}_3)_3$ (0.72 g, 6.4 mmol) dissolved in dry DMF (50 mL) was added dropwise to a mixture of **5** (1.00 g, 2.56 mmol) and diethyl 4-(1,3-dioxane-2-yl)benzylphosphonate (**6**)^[23] (0.788 g, 2.50 mmol) in dry DMF (50 mL). TLC control (SiO_2 , petroleum b.p. 40–70 °C/ethyl acetate, 2:1) indicated the end of the reaction after about 3 h stirring at room temperature. The mixture was poured on crushed ice and the aqueous layer was extracted with CH_2Cl_2 (3 × 50 mL). To the concentrated organic phase (ca. 25 mL) was added CF_3COOH (3.0 mL, 0.039 mol) in H_2O (10 mL). After 2 d stirring at ambient temperature, the mixture was neutralized with NaHCO_3 , washed with a saturated NaCl solution and H_2O and dried with Na_2SO_4 . Evaporation of the solvent yielded 1.00 g (81%) of an orange solid, which melted at 171 °C. ^1H NMR (CDCl_3): $\delta = 0.89$ (t, 6 H, CH_3), 1.30 (m, 12 H, CH_2), 1.57 (m, 4 H, $\beta\text{-CH}_2$), 3.27 (t, 4 H, $\alpha\text{-CH}_2$), 6.60/7.36 (AA'MM', 4 H, arom. H), 6.85/7.10 (AB, $^3J = 16.2$ Hz, 2 H, olefin. H), 7.06/7.24 (AB, $^3J = 16.5$ Hz, 2 H, olefin. H), 7.45/7.48 (AA'BB', 4 H, arom. H),

7.63/7.84 (AA'BB', 4 H, arom. H) ppm. ^{13}C NMR (CDCl_3): δ = 14.0 (CH_3), 22.7, 26.8, 27.3, 31.7 (CH_2), 51.1 (NCH_2), 111.6, 126.2, 126.8, 127.2, 127.9, 130.2 (aromat. CH), 122.8, 126.3, 129.6, 132.1 (olefin. CH), 124.3, 134.6, 135.0, 138.8, 143.7, 148.0 (aromat. C_q), 191.6 (CHO) ppm. FD MS: m/z (%) = 493 (100) [M^+]. HRMS (ESI): calcd. for [$\text{C}_{35}\text{H}_{43}\text{NO} + \text{H}^+$] m/z = 494.3423; found 494.3412.

2,4,6-Tris{(E)-2-[4-(dihexylamino)phenyl]vinyl}-1,3,5-triazine (9): Aldehyde **2** (924 mg, 3.30 mmol) dissolved in dry THF (15 mL) was added dropwise under Ar to 2,4,6-trimethyl-1,3,5-triazine (**8**)^[24] (123 mg, 1.0 mmol) and $\text{KOC}(\text{CH}_3)_3$ (370 mg, 3.3 mmol) in dry THF (15 mL). Stirring at 0 °C was continued for further 30 min, before the temperature was raised to 70 °C. After several days (TLC control: SiO_2 , CH_2Cl_2 /ethyl acetate, 10:1) CH_2Cl_2 (100 mL) was added, and the mixture was carefully washed with saturated NaCl solution and H_2O . After drying with Na_2SO_4 , the volatile parts were evaporated in vacuo and the residue purified by column chromatography (3 × 30 cm SiO_2 , CH_2Cl_2). A red-violet wax (738 mg, 79%) was obtained. ^1H NMR (CDCl_3): δ = 0.89 (t, 18 H, CH_3), 1.31 (m, 36 H, CH_2), 1.59 (m, 12 H, $\beta\text{-CH}_2$), 3.29 (t, 12 H, $\alpha\text{-CH}_2$), 6.61/7.52 (AA'MM', 12 H, arom. H), 6.88/8.14 (AB, 3J = 15.7 Hz, 6 H, olefin. H) ppm. ^{13}C NMR (CDCl_3): δ = 14.0 (CH_3), 22.7, 26.8, 27.3, 31.7 (CH_2), 51.0 (NCH_2), 111.3, 129.9 (aromat. CH), 120.9, 141.3 (olefin. CH), 122.7, 149.3 (aromat. C_q), 171.3 (C-2) ppm. FD MS: m/z (%) = 937 (100) [M^+]. HRMS (ESI): calcd. for [$\text{C}_{63}\text{H}_{96}\text{N}_6 + \text{H}^+$] m/z = 937.7775; found 937.7737.

all-(E)-2,4,6-Tris[2-(4-{2-[4-(dihexylamino)phenyl]vinyl}phenyl)-vinyl]-1,3,5-triazine (10): Aldehyde **5** (489 mg, 1.25 mmol) dissolved in dry THF (10 mL) was added dropwise under Ar to **8** (48 mg, 0.39 mmol) and $\text{KOC}(\text{CH}_3)_3$ (146 mg, 1.9 mmol) in dry THF (20 mL). The reaction mixture was vigorously stirred for at least 1 d at room temperature. Treatment with cold CH_3OH led to the precipitation of the product (343 mg), which contained 2,4-bis[2-(4-{2-[4-(dihexylamino)phenyl]vinyl}phenyl)-vinyl]-6-methyl-1,3,5-triazine and the target compound in a ratio of about 1:1. Column chromatography (2 × 30 cm SiO_2 , toluene) afforded 165 mg (34%) of **10** as a red solid, which melted at 166–167 °C. ^1H NMR (CDCl_3): δ = 0.90 (t, 18 H, CH_3), 1.31 (m, 36 H, CH_2), 1.57 (m, 12 H, $\beta\text{-CH}_2$), 3.27 (t, 12 H, $\alpha\text{-CH}_2$), 6.62/7.38 (AA'MM', 12 H, arom. H), 6.88/7.10 (AB, 3J = 16.2 Hz, 6 H, olefin. H), 7.13/8.24 (AB, 3J = 15.8 Hz, 6 H, olefin. H), 7.50/7.64 (AA'BB', 12 H, arom. H) ppm. ^{13}C NMR (CDCl_3): δ = 14.1 (CH_3), 22.7, 26.8, 27.3, 31.7 (CH_2), 51.0 (NCH_2), 111.6, 126.3, 128.0, 128.6 (aromat. CH), 122.8, 125.3, 130.2, 141.3 (olefin. CH), 124.1, 133.7, 140.1, 148.0 (aromat. C_q), 171.3 (C-2) ppm. FD MS: m/z (%) = 1243 (100) [M^+]. HRMS (ESI): calcd. for [$\text{C}_{87}\text{H}_{114}\text{N}_6 + \text{H}^+$]: 1243.9183; found 1243.9230.

all-(E)-2,4,6-Tris(2-{4-[2-(4-{2-[4-(dihexylamino)phenyl]vinyl}phenyl)vinyl]phenyl}vinyl)-1,3,5-triazine (11): Aldehyde **7** (525 mg, 1.06 mmol), **8** (43 mg, 0.35 mmol) and $\text{KOC}(\text{CH}_3)_3$ (134 mg, 1.2 mmol) reacted as described for **10**. The reaction time was extended to 12 d at room temperature.^[25] The red precipitate (301 mg) obtained by the addition of CH_3OH contained mainly the 1,3,5-triazine with two OPV arms and only a small amount of the target compound. Column chromatography (2 × 30 cm SiO_2 , toluene) yielded 15 mg (3%) of **11** as a red solid, which melted at 97 °C. ^1H NMR (CDCl_3): δ = 0.89 (t, 18 H, CH_3), 1.30 (m, 36 H, CH_2), 1.55 (m, 12 H, $\beta\text{-CH}_2$), 3.26 (t, 12 H, $\alpha\text{-CH}_2$), 6.60/7.36 (AA'MM', 12 H, arom. H, outer ring), 6.85/7.03 (AB, 3J = 16.1 Hz, 6 H, olefin. H, outer double bond), 7.12/7.15 (AB, 3J = 15.8 Hz, 6 H, olefin. H, middle), 7.13/8.24 (AB, 3J = 16.0 Hz, 6 H, olefin. H, inner double bond), 7.35–7.52 (m, 12 H, arom. H), 7.54/7.66 (AA'BB', 12 H, arom. H, inner ring) ppm. ^{13}C NMR (CDCl_3): δ

= 14.1 (CH_3), 22.7, 26.8, 27.3, 31.8 (CH_2), 51.0 (NCH_2), 111.6, 126.2, 126.9, 127.0, 127.8, 128.6 (aromat. CH), 123.0, 125.8, 127.1, 129.1, 129.7, 139.1 (olefin. CH), 124.3, 134.5, 135.9, 138.2, 141.1, 147.8 (aromat. C_q), 171.2 (C-2) ppm. FD MS: m/z (%) = 1550 (100) [M^+]. HRMS (ESI): calcd. for [$\text{C}_{111}\text{H}_{132}\text{N}_6 + \text{H}^+$] 1550.0592; found 1550.0618.

Acknowledgments

We are grateful to the Deutsche Forschungsgemeinschaft, the Fonds der Chemischen Industrie and the Center of Materials Science of the University Mainz for financial support.

- [1] a) H. Meier, *Angew. Chem.* **2005**, *117*, 2536–2561; *Angew. Chem. Int. Ed.* **2005**, *44*, 2482–2506 and references cited therein.
- [2] J. J. Wolff, R. Wortmann, *Adv. Phys. Org. Chem.* **1999**, *32*, 121–217.
- [3] R. E. Martin, F. Diederich, *Angew. Chem.* **1999**, *111*, 1440–1468; *Angew. Chem. Int. Ed.* **1999**, *38*, 1350–1377.
- [4] *Electronic Materials: The Oligomer Approach* (Eds.: K. Müllen, G. Wegner), Wiley-VCH, Weinheim, **1998**.
- [5] H. Meier, in *Carbon-rich Compounds: Molecules to Materials* (Eds.: M. M. Haley, R. R. Tykwinski), Wiley-VCH, Weinheim, **2006**.
- [6] B. R. Cho, K. Chajara, H. J. Oh, K. H. Son, S.-J. Jeon, *Org. Lett.* **2002**, *4*, 1703–1706.
- [7] B. Traber, J. J. Wolff, F. Rominger, T. Oeser, R. Gleiter, M. Gobel, R. Wortmann, *Chem. Eur. J.* **2004**, *10*, 1227–1238.
- [8] H. Meier, H. C. Holst, A. Oehlhof, *Eur. J. Org. Chem.* **2003**, 4173–4180.
- [9] H. C. Holst, T. Pakula, H. Meier, *Tetrahedron* **2004**, *60*, 6765–6775.
- [10] H. Meier, M. Lehmann, H. C. Holst, D. Schwöppe, *Tetrahedron* **2004**, *60*, 6881–6888.
- [11] Y.-Z. Cui, Q. Fang, Z.-L. Huang, G. Xue, G.-B. Xu, W.-T. Yu, *J. Mater. Chem.* **2004**, *14*, 2443–2449.
- [12] Dimethylamino groups are much less favorable; didodecylamino groups are comparably well solubilizing, but lead to lower yields in the synthetic process according to Scheme 3.
- [13] M. Joffre, D. Yaron, R. J. Silbey, J. Zyss, *J. Chem. Phys.* **1992**, *97*, 5607–5615.
- [14] J.-L. Brédas, F. Meyers, B. M. Pierce, J. Zyss, *J. Am. Chem. Soc.* **1992**, *114*, 4928–4929.
- [15] J. Zyss, I. Ledoux, *Chem. Rev.* **1994**, *94*, 77–105.
- [16] I. Ledoux, J. Zyss, J. Siegel, J. Brienne, J.-M. Lehn, *Chem. Phys. Lett.* **1990**, *172*, 440–444.
- [17] J. J. Wolff, D. Längle, D. H. Hillenbrand, R. Wortmann, R. Matschiner, C. Glania, P. Krämer, *Adv. Mater.* **1997**, *9*, 138–143.
- [18] R. Wortmann, C. Glania, P. Krämer, R. Matschiner, J. J. Wolff, S. Kraft, B. Treptow, E. Barbu, D. Längle, G. Görlitz, *Chem. Eur. J.* **1997**, *3*, 1765–1773.
- [19] R. Brettell, D. A. Dunmur, N. J. Hindley, C. M. Marson, *J. Chem. Soc., Chem. Commun.* **1992**, 410–411.
- [20] H. E. Katz, S. F. Bent, W. L. Wilson, M. L. Schilling, S. B. Ungashe, *J. Am. Chem. Soc.* **1994**, *116*, 6631–6635.
- [21] See also A. Hossner, D. Birnbaum, L. M. Loew, *J. Org. Chem.* **1984**, *49*, 2546–2551.
- [22] X. Li, G. Zhang, H. Ma, D. Zhang, J. Li, D. Zhu, *J. Am. Chem. Soc.* **2004**, *126*, 11543–11548.
- [23] See E. Sugiono, H. Detert, T. Metzroth, *Adv. Synth. Catal.* **2001**, *343*, 351–359.
- [24] F. C. Schaefer, G. H. Peters, *J. Org. Chem.* **1961**, *26*, 2778–2784.
- [25] Higher temperatures lead to impurities which are difficult to separate.

Received: January 26, 2006
Published Online: March 31, 2006